Available online at www.sciencedirect.com
SCIENCE DIRECT
Polymer 46 (2005) 4032–4040
polymer
www.elsevier.com/locate/polymer

Relating morphology to nanoscale mechanical properties: from crystalline to mesomorphic iPP

D. Tranchida, S. Piccarolo*

Dipartimento di Ingegneria Chimica dei Processi e dei Materiali, Università di Palermo, Viale delle Scienze, 90128 Palermo, Italy & INSTM UdR Palermo, Italy

Received 8 September 2004; received in revised form 28 December 2004; accepted 16 March 2005
Available online 22 April 2005

Abstract

A nanoindentation technique using an atomic force microscope (AFM) was applied to characterize the mechanical behaviour of several isotactic polypropylene (iPP) samples. The samples were solidified from the melt with a CCT (continuous cooling transformation) procedure spanning a wide range of cooling rates thanks to a fast quenching apparatus developed by the authors. The influence of instrumental parameters on the nanoscale mechanical properties (indentation depth, Young's modulus) shows that for modulus determination one has to rely on simpler methods of force curve analysis based on trace curve alone. Structure homogeneity up to the scale of macroscopic samples used to evaluate elastic moduli allowed a successful comparison of these values with those determined by AFM, which showed that an increase in cooling rate leads to a significant decrease in the material's mechanical response. AFM can thus provide correlations between operating conditions and mechanical properties and can be used for analysing the structure distribution and for mapping properties on a sub-micron scale.
© 2005 Elsevier Ltd. All rights reserved.

Keywords: Mechanical characterization; Nanoindentation; Atomic force microscopy

1. Introduction

Atomic force microscopy makes it possible to study the mechanical properties of materials and to obtain high-resolution images, since it is possible to measure and control tip–surface interaction [1,2]. Quantitative analysis and study of the mechanical behaviour of materials on a nanometer scale becomes feasible with the aid of micromechanical contact models [3–9]. This perspective potentially makes AFM a useful tool for connecting the mapping of properties to the mapping of texture and, in turn, for investigating how processing conditions affect the morphology distribution.

Indentation tests on a nanometer scale, when dealing with polymers, require the use of very low applied loads [1], in the range of 0.5–5 μN. This makes AFM a useful tool, since a few microNewton is the upper limit for this instrument. With respect to nanoindenters, AFM makes it possible to collect images of the sample morphology and to indent specific areas since the AFM sharp tip allows an outstanding lateral resolution. These possibilities turn out to be extremely important when studying inhomogeneous samples (like blends or rubber/matrix systems) or samples with a structure distribution, such as injection moulded samples.

Limitations related to this approach have already been partly discussed in the literature for a variety of polymeric materials ranging from polyurethanes to polystyrene, HDPE–LLDPE mixtures and PET [10–16]. It is required the evaluation of some parameters characterizing the two interacting bodies. Cantilever elastic constant [17] is certainly a fundamental one because AFM measures cantilever deflection, from which one can estimate the applied load. Tip geometry must also be known since entering micromechanical contact models.

The cantilever elastic constant allows to change indentation conditions remarkably: in fact its reduction allows a better force resolution and offers the opportunity to investigate adhesion behaviour, by studying pull-off and jump-to-contact forces [1,18]. On the other hand, increasing the elastic constant offers the opportunity to indent harder materials although it cannot be used for softer ones [10]. So

* Corresponding author. Tel.: +39 91 6567225; fax: +39 91 6567280.
E-mail address: piccarolo@unipa.it (S. Piccarolo).

0032-3861/$ - see front matter © 2005 Elsevier Ltd. All rights reserved.
doi:10.1016/j.polymer.2005.03.055

the cantilever elastic constant has to be carefully chosen, depending on the latitude of the physical properties of the materials under study [19].

As far as knowledge of the tip geometry is concerned, manufacturer data are often not sufficient because of production scatter. Moreover, upon making a force curve analysis with large tip penetrations significant modifications can arise in the tip geometry due to residues of the material under study being removed and deposited on the tip and, under drastic conditions of use, due to tip damage and wear [20]. Tip condition can be characterized in terms of apex curvature radius. Although being in the order of 10 nm, it is difficult to measure even by electron microscopy. Despite the crucial role of the tip radius in characterizing mechanical properties through indentation tests, this quantity is seldom reported. However, methods such as blind estimation [21] can be used for routinely estimating changes in tip geometry.

All things considered, contact models can only be applied if these parameters are known. The three most frequently used models in the literature are Oliver–Pharr, Hertz and JKR/DMT. The first [4] requires a double calibration by indentations performed on a reference material, usually aluminium, tungsten or silicon, and it is based on the hypothesis of a purely elastic unloading recovery. The Hertz model [5] relates mechanical properties to tip penetration depth into the material assuming a purely elastic contact. The DMT [6] and JKR [7] models are based on the Hertz approach but introduce corrections due to adhesion forces.

Recently Arivuoli et al. have reported a model [9] based on energetic considerations in which elastic and plastic work estimates provide the elastic modulus in addition to other interesting parameters linked to the influence of plasticity on indentation.

The purpose of this work is to measure, through nanoindentation, the mechanical response of several isotactic polypropylene (iPP) samples solidified by a continuous cooling transformation (CCT) approach in a wide range of cooling rates, using an apparatus recently introduced by the authors [22,23], thus emulating typical polymer processing solidification conditions.

In the nanoindentation technique the AFM was used as an indenter recording the so-called force-curve plots (i.e. applied load vs. penetration depth) under different experimental conditions (frequency, i.e. penetration rate and load) for samples quenched at different cooling rates and displaying a wide range of properties. Subsequently these force-curve plots were interpreted using force curve analysis methods reported in the literature, so as to determine Young's modulus values. The calculated mechanical properties were then related to the solidification conditions (namely the cooling rate) in order to establish reliable structure–property relationships.

2. Experimental section

2.1. Material and experimental technique

The material used was isotactic polypropylene (trade name T30G) with $M_n = 75{,}100$, and $M_w/M_n = 6.4$, kindly provided by Himont. It was crystallized from the melt at four different cooling rates (2.5, 25, 110 and 350 °C/s) according to a procedure fully described elsewhere [22]. Film thickness was in the order of 50 μm, ensuring that we were measuring bulk film properties [24].

Force curves and topographic images were obtained with a Digital Instruments Nanoscope IIIA Controller. Silicon tapping cantilevers were used in order to be able to carefully choose the area of the sample where to perform indentations, take post-indentation images and, in some cases, study their time evolution.

Nanoindentations were performed at various loads, frequencies and, consequently, penetration rates. Loads ranged from approx. 0.7 to 4 μN; the lower bound was determined by the occurrence of unstable results while above the higher bound cantilever deflection is saturated so that larger loads are not allowed due to the non-linear response of the system. Although stiffer cantilevers could be used to expand the allowable loads range, most of the information on the occurring mechanisms are obtained with the single standard cantilever.

Frequencies, (at a fixed ramp size of 900 nm) covered four orders of magnitude, from 0.01 to 100 Hz. It is worth remembering that 10 Hz is then equivalent to a penetration rate of 18 μm/s, and 0.01 Hz to 18 nm/s. It is assumed that such a rate is constant throughout the piezo scanning since the wave form applied to the piezo is, to a good approximation, a saw tooth if one excludes inertia effects which are frequency dependent and mostly located around the inversion point of the piezo scanning.

2.2. Sample preparation

Summarizing, a continuous cooling transformation (CCT) approach like the one widely used in metallurgy was adopted, allowing structure–thermal history quantitative relationships to be assessed through post-mortem investigation of sample morphology (Optical microscopy, wide-angle X-ray diffraction (WAXD), infra red (IR) spectroscopy) and properties (density and microhardness) [22,24]. Fig. 1 shows the dependence of density and WAXD on the cooling rate for the material under investigation. The samples investigated here cover 2 decades of cooling rates hence, according to previous authors' observations, a continuous variation of mechanical properties is expected showing a strong dependence of crystallinity, density and microhardness on cooling rate [22,23,25].

As a matter of fact, owing to the CCT procedure adopted, all samples exhibit the peculiarity of being solidified under conditions emulating polymer processing. Under these

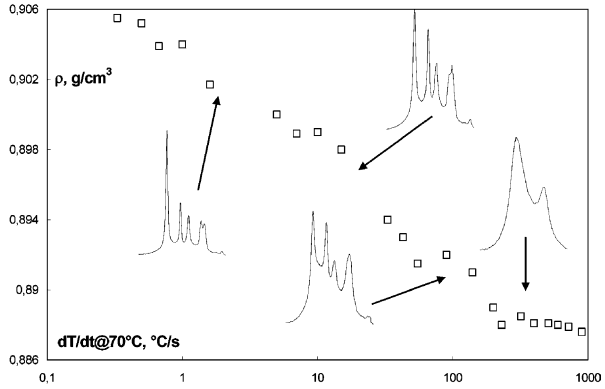

Fig. 1. CCT behaviour of the iPP under investigation as obtained by the density vs. cooling rate characteristic. Selected WAXD patterns are also shown.

circumstances solidification gives rise to a metastable crystalline structure that is farther removed from thermodynamic equilibrium at higher cooling rates [22]. In particular, cooling rates of 350 °C/s correspond to the onset of the metastable mesomorphic structure of iPP [23,25], 2.5 and 25 °C/s give rise to the onset of the stable α-monoclinic phase of iPP with a fully spherulitic morphology and 110 °C/s, for the particular iPP used in this work, corresponds to the dispersion of α-monoclinic spherulites in a mesomorphic phase matrix [23,25].

It should also be emphasized that the aforementioned experimental procedure of sample preparation ensures complete structural homogeneity as revealed by micrometric resolution techniques [23,25] (optical microscopy, density, micro hardness, WAXD).

Samples were prepared with the cited CCT procedure between two microscope cover glasses in order to obtain low roughness as confirmed by the possibility of choosing a very smooth and homogeneous zone for indentation upon imaging the sample in tapping mode and phase contrast in air. Microroughness (calculated within a 1×1 μm^2 area) was in the range of 1.4–5.9 nm and fractal dimension in the range 2.62–2.83. Thus, all surfaces studied were smooth, with random variation of elevations.

Residual stresses are quickly relaxed after sample preparation since T_g of iPP is around 263 K; however, in order to prevent subsequent structural modifications due to the metastable nature of the material solidified under such conditions, samples were kept at 243 K between indentation tests [26].

Standard tensile test experiments were also performed in a previous study [27] using standard equipment (Instron testing machine model 1122), in order to compare nanoscale Young's Modulus values to macroscopic ones. Non-standard tensile samples with dimensions of $30\times5\times0.2$ mm^3 and a crosshead speed of 5 mm/min were used.

2.3. Data analysis method

In order to properly analyse AFM force-curve plots, in particular to achieve a repeatable evaluation of the elastic modulus, a number of prerequisites must be met. First of all, the value of the cantilever elastic constant should be carefully determined, as will be outlined below. Second, knowledge of some geometrical parameters is necessary to implement the contact models used to calculate material mechanical behaviour on a nanoscale. Finally, some basic definitions will provide a better understanding of the phenomenology occurring during AFM nanoindentation omitting however the details reported in a recent review [1].

We define indentation as the depth of the tip residual imprint measured on the sample by a topographic scan performed after the force curve is recorded, whereas we define penetration as the tip maximum measured penetration depth, as registered from the force curve. Penetration and indentation differ because during unloading the sample elastically returns so that indentation is always smaller than (maximum) penetration. In polymer samples indentation usually continues to decrease with time, and may eventually vanish at very long times depending on sample characteristics [28]. A quantitative account of this behaviour is however beyond the scope of this work.

Thus penetration, as determined in this work, is indeed due to the instantaneous sample response to the load increasing to its maximum applied value during a trace of the piezo scan at a given rate.

The elastic contact model due to Hertz [1,5] does not consider adhesion forces between the interacting bodies and it assumes contact between two elastically deforming spheres. Setting one of the radii to infinite, the penetration of a sphere into a plane is obtained. The relationship with Young's modulus is:

$$E = \frac{3(1-\nu^2)}{4}\frac{F}{R^{1/2}h^{3/2}} \tag{1}$$

where F is the applied load, R the tip curvature radius, E the sample elastic modulus, n the sample Poisson ratio, h the penetration depth. The relationship remains the same in the case of a paraboloid in contact, by a finite contact area, with a half-space, as was shown by Sneddon [3].

The tip is sometimes modelled as a pyramid or as a cone with an equivalent opening angle. In this case a simple dimensional analysis leads to a power law relation between applied load and penetration depth, the exponent being equal to 2, confirmed by numerical simulations [29] and theory [3].

In the case of AFM nanoindentation with small penetration depths, the comparable tip curvature radius leans on the introduction of this radius as a suitable length scale. The exponent, no longer equal to 2, turns out, experimentally, to be very close to 1.5, again in agreement with theoretical predictions by Sneddon [3].

The slope of the unloading curve, corrected for instrumental contributions, is used in the Oliver–Pharr method to calculate the elastic modulus [5]. A double calibration has to be performed on a reference material, usually tungsten or fused silica, to determine the load-frame compliance and the tip area function.

One may note from the force curves reported in Fig. 2 that adhesion, pointed out by the negative portion of cantilever deflection, decreases with frequency [30,31]; moreover it is worth remembering that adhesion increases with the applied load [31]. This raises doubts about the applicability of the Hertz model for modulus calculation, particularly at low frequencies and larger loads. Following Johnson [32] one can estimate that the operating conditions used in this work are at the boundary between the Hertz model and the DMT model. Although it is true that the DMT model accounts for phenomena that are not explicitly accounted for in the Hertz model, it could be shown that, under these conditions, it yields results that are very similar, with an error of approx. 5% in the worst operating condition, i.e. lower frequency and larger applied load. For this reason its application has been omitted in the rest of the discussion since an account of adhesion significantly complicates the model formulation without leading to a significant improvement in modulus prediction.

Arivuoli et al. [9] instead adopted an energetic approach, assuming that during a force curve, piezo displacement upon contact, is the sum of an elastic-like and a plastic-like contribution.

The elastic contribution is calculated through the elastic work, which is assumed to be the integral of the unloading force curve vs. piezo displacement. The plastic-like contribution can be derived from the area between the loading and unloading curves. By dividing this parameter by a geometric coefficient relating penetration to the cross-sectional area of the imprint one gets the material hardness parameter, through which the elastic modulus can be evaluated [9].

The application of the above-mentioned methods requires a good knowledge of the two interacting bodies' geometries, i.e. knowledge of the tip curvature radius, modelled as a paraboloid, and the sample surface, modelled as a half-space, which must be flat enough on the indentation scale. Furthermore, the cantilever elastic constant must be measured with good accuracy to work out the applied load from the cantilever deflection.

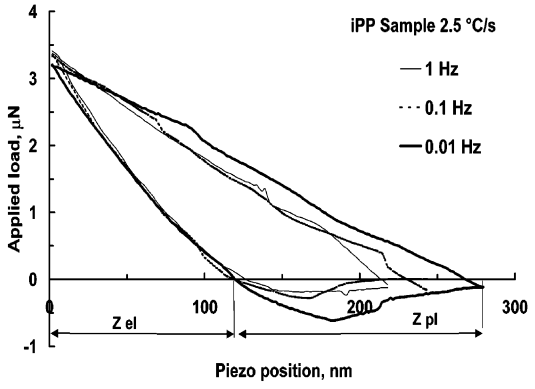

Fig. 2. Typical force curve plots for the samples studied in this work, obtained at 0.1, 1, 10 Hz.

The tip curvature radius was in the range of 5–10 nm as provided by the producer. Its use ensures a very high lateral resolution in mechanical characterization with respect to Berkovich type indenters. Tip geometry blind estimates were performed from time to time by imaging an aluminium membrane, used as tip-characterizer sample, with a scan size of 500 nm, at a scan frequency of 0.8 Hz, with a resolution of 512×512 pixel [20]. These estimates were used for tip qualification in force curve analysis and gave results very similar to the producer's data. Results reported elsewhere [33], achieved through tip profile deconvolution from the image of gold nanospheres with radii comparable to that of the tip, show a good agreement with the values of tip radii we obtained.

Cantilever deflection is related to the instantaneous force applied if the cantilever elastic constant, k, is known. Its determination is very important because deviations from the nominal value supplied by the producer may typically amount to ±200% when thinner cantilevers are used [17]. This error heavily reflects on the evaluation of the load applied in nanoindentation. The elastic constant of the cantilevers used in this work has a nominal value, provided by the producer (DI Inc., Santa Barbara CA), of ∼30 N/m. In every case this has been confirmed experimentally, according to the procedure described by Tsukruk [17] by measuring the cantilever natural resonance frequency and combining this with the geometric parameters as revealed by a cantilever SEM image. Theoretical solution of the mechanical problem has often been used to estimate the cantilever elastic constant [34–38]. This turns out to be accurate if a rectangular single beam one component cantilever is used, whereas for V-shaped cantilevers a precision of ±25% is attained [1,17]. The procedure consists in measuring the cantilever resonance frequency to estimate its thickness. Thus, one gets, for k (N/m):

$$k = \frac{3EI}{L^3} \tag{2}$$

where L and I are the cantilever's length and cross-sectional (trapezoid) moment of inertia, respectively. Deviations from the nominal value of up to 20% were observed due to the use of tapping mode cantilevers. FEM simulations showed that the method is in very good agreement with numerical simulations (less than 1% difference).

3. Results

Fig. 3 shows a comparison between indentation scale and texture for an iPP sample solidified at 110 °C/s:

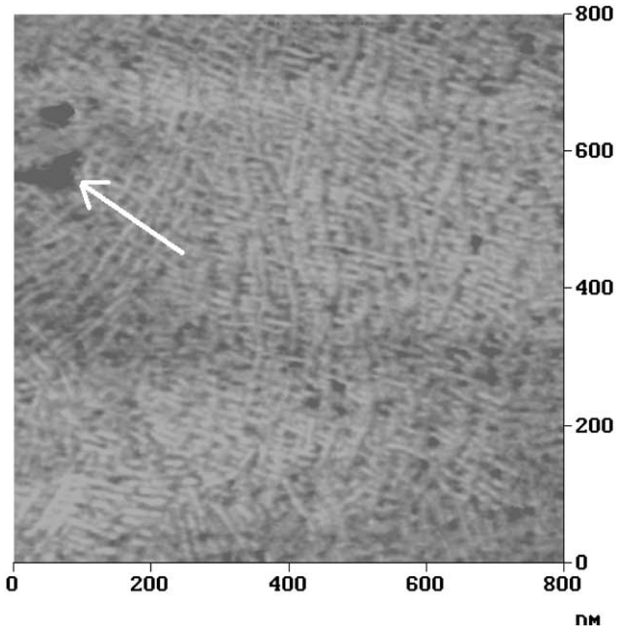

Fig. 3. Nanoscale mechanical test: crosshatched lamellae in the 110 K/s sample compared with typical indentations pointed out by arrow. Applied load was 3.02 μN.

crosshatched lamellae are clearly visible, together with an indentation residual imprint. The nanoscale mechanical properties, arising from nanoindentation, are determined by morphology on a very local scale since few lamellae are involved.

The typical force curves, shown in Fig. 2, provide the instantaneous cantilever deflection vs. piezo position. They are representative of the material's mechanical behaviour through the penetration dependence on applied load, function, also, of loading geometry and frequency. Taking images immediately after the force curve one can measure the residual imprint depth, i.e. indentation, and compare it to the maximum penetration depth, as measured by the abscissa in the force curve. The ratio of these two quantities, always smaller than one, can be assumed as a plasticity parameter. It is shown in Fig. 4 for 2.5 and 350 °C/s samples and clearly depends on frequency and material response. Material behaviour is closer to pure elastic response, plasticity index equal to zero, at high frequency: the recovery is very pronounced at 10 Hz and the force curve thus occurs mostly within the material's elastic response.

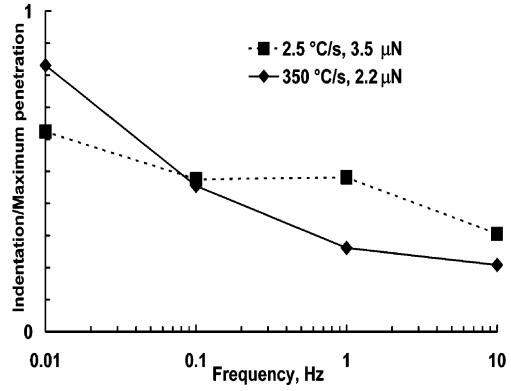

Fig. 4. Indentation, i.e. permanent deformation, divided by penetration depth of tip indenter vs. frequency for samples solidified at extreme conditions (2.5 and 350 °C/s).

A typical plot of penetration depth as a function of frequency is shown in Fig. 5 under different loading conditions. It is clear from the figure that penetration decreases with increasing loading rate at a constant applied load. However, within the range tested, the load does not influence the frequency dependence of the penetration measured. Therefore a compliance parameter, obtained by dividing the final penetration by the applied load, proves to be independent of the applied load. Moreover, a comparison of the compliance parameters of different samples shows that the sample cooled at 2.5 °C/s is stiffer than the one cooled at 25 °C/s, which in its turn is stiffer than the samples solidified at 110 and 350 °C/s, i.e. with decreasing crystallinity as reported in Fig. 1. Finally, Fig. 5 shows that the sample compliance, decreases with increasing sample crystallinity.

These findings are in full agreement with previous authors' observations showing that bulk microhardness continuously and gradually decreases with the cooling rate [39] and therefore increases with increasing crystallinity.

Contact mechanics models, available in the literature and already briefly summarized above, are needed to translate these observations into quantitative information, i.e. into elastic modulus values. Previous works [10,16] examined and compared the Oliver–Pharr, Hertz and JKR methods, showing that for indentations that are 'not too moderate', i.e. indentations for which the instability of the contact and the presence of superficial forces causes the elastic modulus to oscillate by more than an order of magnitude, they all lead to satisfactory predictions of the elastic modulus. The threshold of the indentation adopted was found to be approx. 20 nm in those experimental conditions. In other

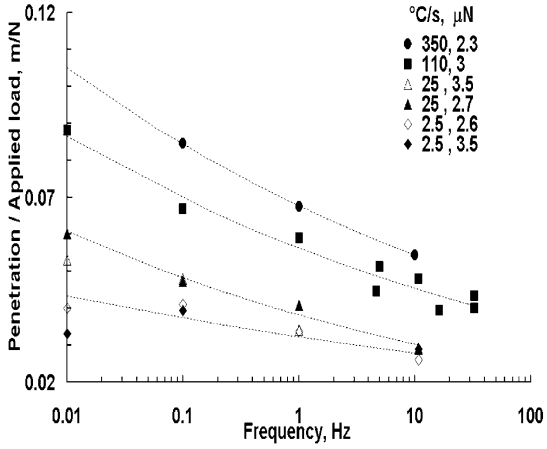

Fig. 5. Frequency dependence of compliance parameter drawn from ratio of maximum penetration on load. Lines are a guide for the eye.

words, this experimental observation defines a lower bound for the size range in which it is possible to perform a quantitative material mechanical characterization by indentation on the nanoscale.

In the case of the Oliver–Pharr method the first difficulty arises in the application of the double calibration since the AFM cantilever cannot indent typical reference materials [10]. However the use of softer materials is questionable, as it has been shown that calibration results are significantly affected by the reference chosen [40]. Moreover, in this particular case (using AFM force curves), the use of a softer material for the double calibration means that the most important information is missing since the unloading curves are always superimposed, as Fig. 2 shows, and are apparently independent of the frequency and even of the material's mechanical properties, as it will be shown in the following.

Fig. 6 shows the dependence of z_{el}/F, i.e. z_{el} normalized by applied load, on the reciprocal cantilever elastic constant for four different cantilevers used to analyse different samples. This figure provides a quantitative interpretation of this behaviour: the filled points represent the average z_{el}/F obtained for different frequencies (from 0.1 up to 10 Hz) and different applied loads (from 0.7 to 4 μN) and the bars correspond to the standard deviation. Since the data points refer to different samples and frequencies, it is clear that z_{el} does not depend on them and therefore does not depend on the material's mechanical response either.

This suggests that z_{el}, under the broad range of experimental conditions used and sample properties, is not a material feature but depends on instrumental characteristics, i.e. on the cantilever elastic constant, as the data in Fig. 6 clearly show.

The explanation relies on the fact that the retrace part of the force curve is not really obtained unloading the sample but moving the sample away from the tip. In this way, the cantilever deflection decreases of an amount that is in any case equal to the piezo displacement and the retrace is only controlled by cantilever stiffness. For indentation on rubbers the loading and the unloading curves are however superimposed, this suggests that in this case either inverse plasticity phenomena occur [41] or that piezo retrace time in the above range of frequencies is smaller than iPP minimum relaxation time, as expected for a viscoelastic solid. This observation, which limits the use of force curves analysis in this context, needs however to be further investigated.

In addition, this result shows that elastic modulus dependence on frequency and cooling rate is to be found in z_{pl}. This observation points to a serious limitation of AFM force curves and casts doubt on the applicability of methods using the retrace curve (i.e. the unloading portion of the force curve) for modulus calculation.

The possibility of using the trace curve alone for modulus calculation must thus rely on simpler models of contact mechanics. The method of Arivuoli et al. [9] makes it possible to estimate the mechanical work done by the cantilever on trace and retrace during a piezo scan from the force curve and filters the retrace work arising from cantilever elastic deformation. On the other hand, by adopting the Hertz method, based on a force balance and making use of actual penetration only, the elastic modulus can be calculated from the trace curve only.

Use of the Hertz method seems however an apparent contradiction since elastic properties can be obtained only from the trace portion of the force curve, where the mechanism of indentation is apparently far from being purely elastic (or viscoelastic), permanent plastic deformations may well play a significant role particularly with small tip radii [42] and impact fracture may be important for high indentation frequencies [43].

Fig. 7 shows elastic modulus results calculated using the approaches of Hertz and Arivuoli et al. The uncertainty in the calculation by the Hertz method is mostly related to the blind estimate of the tip radius, but tip radii values between 5 and 10 nm give rise to an error which provides values of

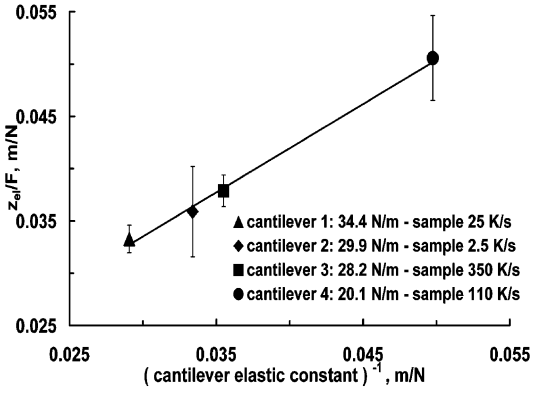

Fig. 6. Cantilever elastic recovery, drawn from retrace AFM force curve, normalized by load, vs. reciprocal cantilever elastic constant. Data points taken at different frequencies and sample thermal histories are compared to a linear fitting.

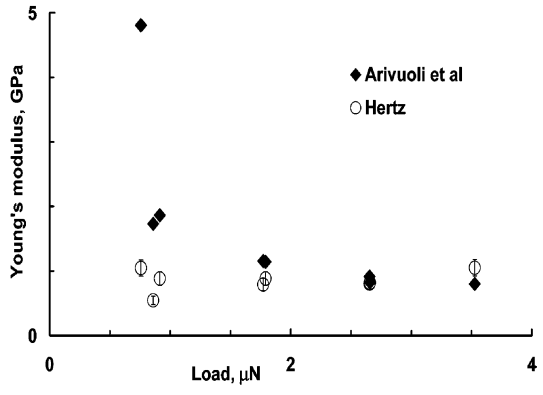

Fig. 7. Dependence of nanoscale elastic modulus on load for an iPP sample solidified at 2.5 °C/s. Moduli are calculated from force curve analysis using the models of Hertz and Arivuoli (see text). Error bar for Hertz modulus is obtained using tip radii of 5 and 10 nm.

moduli in good agreement with those provided by the energetic approach of Arivuoli et al.

In both cases a lower bound for the applied force is apparent from the increased scatter in the value of the modulus. Although in the case of the Hertz model this threshold is the same as observed in the cited papers [1,10,16] this must be a coincidence since this lower load bound should not be an absolute threshold but should depend on a combination of sample roughness and tip sharpness [44] other than on penetration depth, which is in its turn dependent on material properties. A decrease of the elastic modulus on increasing penetration depth, as well as the decrease of hardness, was shown to be a strain rate effect [45] due to the decreasing strain rate with increasing penetration depth. This explanation is however questionable as Hochstetter et al. [41] showed that it was an artefact from calculation and it was possible to get rid of it changing the loading history.

It is relevant to observe that, for both methods, elastic modulus calculation does not depend on the applied load if this is above the lower bound. Given the complex mechanism of indentation by the AFM tip, it would be likely to relate this event to the possibility that elastic behaviour dominates the deformation mechanism.

By performing indentations at various frequencies one can observe a frequency dependent behaviour of the elastic modulus similar to the one shown by the penetration depth as a function of frequency in Fig. 5. Fig. 8 shows the frequency dependence of the elastic modulus determined with the aid of the Hertz and Arivuoli et al. models for the 25 °C/s sample. It is clear that the elastic modulus results depend not only on the penetration depth but also, and similarly, on the penetration rate, i.e. on the frequency: apparently the modulus increases with increasing frequency and the material is stiffer. It is questionable, however, to relate the frequency dependence of elastic modulus to the material's viscoelastic behaviour [21] since the range is much wider than usually reported for iPP [46]. This was already shown in the literature [41] on other systems, i.e.

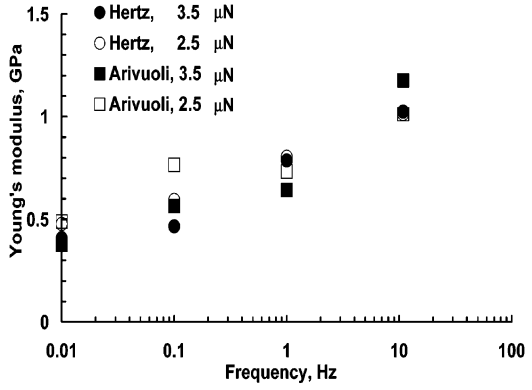

Fig. 8. Frequency dependence of nanoscale elastic modulus obtained from force curve with Hertz and Arivuoli models, 25 °C/s sample (see text for details).

increasing the loading rate a surprisingly strong change in mechanical properties, albeit not explained, takes place. Although it should be mentioned that an increase of moduli is observed in conjunction with decreasing holding times [47,48], this strategy cannot be adopted since Nanoscope IIIA cannot apply a constant load at the end of loading. Furthermore the material's mechanical behaviour is very complex under the large strains localized at the tip interface and the time dependent behaviour may be masked by a frequency dependence of piezo hysteresis and piezo sensitivity [44], thus decoupling material behaviour from instrumental characteristics may be a difficult task and as a consequence the same also holds for obtaining a meaningful elastic modulus frequency dependence from AFM nanoindentation measurements.

Fig. 9 shows a comparison between the macroscopic determination of the elastic modulus and the 'nanoscale' elastic modulus as determined by the force curve method using the approach of Arivuoli et al. The macroscale modulus and the nanoscale modulus are comparable at frequencies of 10 Hz. It is worth noting that, taking into account the ramp size (900 nm) and assuming the piezo is driven by a saw tooth, a frequency of 10 Hz corresponds to a piezo scanning rate of 18 μm/s, similar in magnitude to the overall deformation rate of the tensile testing apparatus, which equals approx. 8.3 μm/s (i.e. 0.5 mm/min [27]).

This result, although it is in line with previous determinations of the elastic modulus by AFM [10–15] is somewhat surprising since local and overall deformation rates in the macroscopic tests may be different: first of all samples used for macroscopic tests were not dumbbell shaped since the size of the original quenched samples is very small, secondly one may question whether the reciprocity of mechanical properties in tension and compression applies in this case, and finally the deformation geometry in the force curve test is not of pure compression nor is a constant strain rate applied.

Although the correspondence between the 'nanoscale' elastic moduli reported in Fig. 9, and those determined

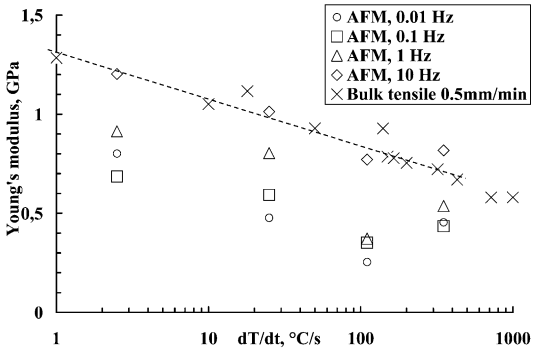

Fig. 9. Cooling rate dependence of elastic modulus for the iPP under investigation. Crosses refer to Young's moduli from tensile tests on macroscopic samples where the line drawn is a guide for the eye. Open symbols refer to moduli obtained from force curve analysis by Arivuoli model (see text) at different frequencies.

'macroscopically' may be fortuitous, i.e. due to compensation mechanisms that are not fully understood yet, Fig. 9 certainly shows that the relative magnitude of moduli in dependence of different morphologies is fully acknowledged. This makes it possible to perform in situ mechanical analysis with very low lateral resolution. Unlike conventional analysis techniques, AFM can thus provide correlations between operating conditions and mechanical properties and can serve as a tool for analysing the structure distribution and for property-mapping on a sub-micron scale.

This result relies on the material to be continuous and isotropic on the scale of the indentation size, and therefore on the use of samples that are homogeneous up to the size used for the macroscopic tensile tests. Thus it is a further proof that the CCT procedure developed indeed yields homogeneous samples on the scale of their macroscopic geometrical dimensions, provided that some constraints for the solidification procedure are met [22]. In previous works the technique of force curve analysis for modulus determination has been applied in a variety of conditions on samples ranging from polyurethanes to polystyrene, HDPE–LLDPE mixtures and PET, without this problem ever having been mentioned [10–15].

4. Conclusions

In this work an AFM nanoindentation technique was applied to iPP samples solidified with a CCT procedure under different cooling rate conditions from 2.5 to ca 300 °C/s yielding homogeneous samples ranging from α-monoclinic semicrystalline to mesomorphic.

Other than penetration in dependence of sample thermal history, Young's modulus can be drawn from force curve analysis although using simple methods since the retrace curve is not dependent on material characteristics but is only related to the cantilever elastic constant.

The nanoscale moduli were evaluated by a traditional force balance model (Hertz) and by a model based on an energy balance recently proposed in the literature (Arivuoli et al. [9]). They are close to each other and to the moduli obtained in a macroscopic tension test on full size samples (i.e. a few mm), provided that comparable 'overall' deformation rates are used (approx. 10^{-5} m/s).

Thus samples homogeneity, provided by the technique adopted for sample preparation, allows a comparison of nanometer scale data and bulk. Although the frequency dependence of the tip penetration depth and the elastic moduli shows the expected trend, a material's viscoelastic behaviour cannot be determined by such measurements due to coupled instrumental time dependent features and the complexity of the deformation mechanism.

Although the correspondence between nanoscale and bulk moduli might be due to a fortuitous compensation of these effects, nanoscale moduli decrease with increasing cooling rate according to a relationship that closely resembles the relationship found for bulk samples.

This first of all confirms that the samples used are homogeneous up to the size used for the macroscopic tensile tests and shows that surface effects on this scale on iPP are not relevant. A further consequence of these observations suggests that the complexity of the deformation mechanism under the tip of the indenter might be simply reconciled with the large elastic (or viscoelastic) range of semicrystalline materials and in particular of iPP notwithstanding the wide latitude of morphologies analysed.

These results open the possibility for using AFM force curves information as a tool for structure mapping and thus provide correlations between operating conditions and mechanical properties on the nanoscale.

Acknowledgements

We gratefully acknowledge the support of the PhD fellowship of DT by the University of Palermo. The authors wish to acknowledge enlightening and stimulating discussions with Dr Rudy Deblieck of Resolve-DSM Research.

References

[1] Cappella B, Dietler G. Surf Sci Rep 1999;34:1–104.
[2] Jandt KD. Mater Sci Eng 1998;R21:221–95.
[3] Sneddon IN. Int J Eng Sci 1965;3:47–57.
[4] Oliver WC, Pharr GM. J Mater Res 1992;7(6):1564–83.
[5] Landau LD, Lifshitz EM. Theory of elasticity. Oxford: Pergamon Press; 1986. p. 43.
[6] Derjaguin BV, Muller VM, Toporov YP. J Colloid Interface Sci 1975; 53:314–26.
[7] Johnson KL, Kendall K, Roberts AD. Proc R Soc London 1971;A324: 301–13.
[8] Maugis D. J Colloid Interface Sci 1992;150:243–69.
[9] Arivuoli D, Lawson NS, Krier A, Attolini G, Pelosi C. Mater Chem Phys 2000;66:207–12.
[10] Tsukruk VV, Huang Z, Chizhik SA, Gorbunov VV. J Mater Sci 1998; 33:4905–9.
[11] Herrmann K, Jennett NM, Wegener W, Meneve J, Hasche K, Seemann R. Thin Solid Films 2000;377–378:394–400.
[12] Bischel MS, VanLandingham MR, Eduljee RF, Gillespie JW, Schultz JM. J Mater Sci 2000;35:221–8.
[13] Du B, Liu J, Zhang Q, He T. Polymer 2001;42:5901–7.
[14] Tsukruk VV, Sidorenko A, Yang H. Polymer 2002;43:1695–9.
[15] Beake BD, Leggett GJ. Polymer 2002;43:319–27.
[16] Chizhik SA, Huang Z, Gorbunov VV, Myshkin NK, Tsukruk VV. Langmuir 1998;14:2606–9.
[17] Hazel JL, Tsukruk VV. Thin Solid Films 1999;339:249–57.
[18] Hao HW, Barò AM, Saenz. J Vac Sci Technol B 1991;9:1323–8.
[19] Tsukruk VV, Gorbunov VV, Huang Z, Chizhik SA. Polym Int 2000; 49:441–4.
[20] Khurshudov A, Kato K. Ultramicroscopy 1995;60:11–16.
[21] Villarrubia JS. J Res NIST 1997;102:425–54.
[22] Brucato V, Piccarolo S, La Carrubba V. Chem Eng Sci 2002;57: 4129–43.
[23] Piccarolo S, Saiu M, Brucato V, Titomanlio G. J Appl Polym Sci 1992;46:625–34.

[24] Saha R, Nix WD. Acta Mater 2002;50:23–38.
[25] Piccarolo S. J Macromol Sci Phys B 1992;31(4):501–11.
[26] Martorana A, Piccarolo S, Sapoundjieva D. Macromol Chem Phys 1999;200:531–40.
[27] Gerosa A. Proprietà meccaniche e morfologia di polimeri cristallini in funzione della velocità di raffreddamento. Laurea Thesis, Università di Palermo, Faculty of Engineering; 1996.
[28] Karapanagiotis I, Evans DF, Gerberich WW. Polymer 2002;43: 1343–8.
[29] Cheng YT, Li Z, Cheng CM. Phil Mag 2002;A82:1821–9.
[30] Aimè JP, Elkaakour Z, Odin C, Bouhacina T, Michel D, Curely J, et al. J Appl Phys 1994;76:754–62.
[31] Pickering JP, Vancso GJ. Macromol Symp 2001;167:189–99.
[32] Johnson KL, Greenwood JA. J Colloid Interface Sci 1997;192: 326–33.
[33] Ramirez-Aguilar KA, Rowlen KL. Langmuir 1998;14:2562–6.
[34] Sader JE. Rev Sci Instrum 1995;66:4583–7.
[35] Albrecht TR, Akamine S, Carver TE, Quate CF. J Vac Sci Technol A 1990;8:3386–96.
[36] Neumeister JM, Ducker WA. Rev Sci Instrum 1994;65:2351–527.
[37] Sader JE, Larson I, Mulvaney P, White LR. Rev Sci Instrum 1995;66: 3789–98.
[38] Senden T, Ducker W. Langmuir 1994;10:1003–4.
[39] La Carrubba V, Brucato V, Piccarolo S. J Polym Sci, B Polym Phys 2002;1:153–75.
[40] Jennett NM, Meneve J. Fundamentals of nanoindentation and nanotribology. 522. Pittsburgh, PA: Materials Research Society; 1998. p. 239.
[41] Hochstetter G, Jimenez A, Loubet JL. J Macromol Sci Phys 1999; B38:681–8.
[42] VanLandingham MR. J Res NIST 2003;108:249–65.
[43] Mann AB, Pethica JB. Phil Mag 1999;A79:577–92.
[44] VanLandingham MR. Microsc Today 1997;97:12–15.
[45] Beake BD, Chen S, Hull JB, Gao F. J Nanosci Nanotechol 2002;2: 73–9.
[46] Mc Crum NG, Read BE, Williams G. Anelastic and dielectric effects in polymeric solids. London: Wiley; 1967. p. 377.
[47] Flores A, Baltà Calleja FJ. Phil Mag 1998;A78:1283–97.
[48] Wolf B. Cryst Res Technol 2000;35:377–400.